Stereologic Characterization and Spatial Distribution Patterns of Betz Cells in the Human Primary Motor Cortex

CLAIRE-BÉNÉDICTE RIVARA,[1,2] CHET C. SHERWOOD,[2,5,6] CONSTANTIN BOURAS,[1,2] AND PATRICK R. HOF[2–4,6]*

[1]Department of Psychiatry, Neuropsychiatry Division, HUG Belle-Idée, University of Geneva School of Medicine, Geneva, Switzerland
[2] Kastor Neurobiology of Aging Laboratories and Fishberg Research Center for Neurobiology, Mount Sinai School of Medicine, New York, New York
[3]Department of Geriatrics and Adult Development, Mount Sinai School of Medicine, New York, New York
[4]Department of Ophthalmology, Mount Sinai School of Medicine, New York, New York
[5]Department of Anthropology, Columbia University, New York, New York
[6]New York Consortium in Evolutionary Primatology, New York, New York

ABSTRACT

Betz cells are giant motoneurons located in layer Vb of the primate primary motor cortex. We conducted stereological analyses of Betz cells and neighboring pyramidal cells from the brains of six neurologically normal elderly humans to determine their volume, total number, and spatial distribution, and to relate these data to functional localization. The distribution of cellular volumes exhibits a bimodal pattern, delineating two different subpopulations. Betz cell volumes follow a mediolateral gradient, the largest Betz cells being located on the most medial part of the motor cortex. Additionally, the shape of Betz cells varies between the rostral and caudal parts of the primary motor cortex, supporting the notion that there are anatomically distinct zones in primary motor cortex. The total number of Betz cells per hemisphere accounts for about one-tenth of the total number of pyramidal cells in layer Vb. Analysis of spatial distribution using Voronoi tessellation revealed maximal clustering of Betz cells in a zone situated two-thirds from the midline along the mediolateral axis of the primary motor cortex. These data suggest that Betz cells have a discrete subregional distribution that may correspond to certain aspects of the functional parcellation of area 4. These results may offer a histological correlate of functional imaging studies and are relevant in the context of neurodegenerative diseases such as amyotrophic lateral sclerosis, progressive supranuclear palsy, and Guamanian amyotrophic lateral sclerosis/Parkinsonism-dementia, and in studies of normal brain aging. Anat Rec Part A 270A:137–151, 2003.

Key words: amyotrophic lateral sclerosis; area 4; Betz cells; cytoarchitecture; human neocortex; motoneurons; stereology

The human neocortex is characterized by regional and laminar specific distributions of a variety of neuronal subtypes and distinct afferent and efferent connections. The neocortex can be parcellated into a large number of more or less distinct fields according to microscopic architecture. Identification of the primary motor cortex and its boundaries, however, has been particularly contentious. Brodmann (1903, 1909) originally described area 4 as an agranular zone, delineated by the presence of Betz cells, a subpopulation of giant infragranular pyramidal neurons in cortical layer V, located on its rostral border and buried in the depth of the anterior wall of the central sulcus. This definition has since been criticized (Zeki, 1979), and Brodmann's original delineation of the primary motor cortex has been revised by other investigators, who described an intermediate precentral area, an area precentralis A, area FAγ (von Economo and Koskinas, 1925), area 42 (Vogt and Vogt, 1926), area 4γ (agranular, containing the Betz cells),

Grant sponsor: NIH; Grant numbers: AG05138; AG14382; MH58911; Grant sponsor: NSF; Grant number: BCS-0121286; Grant sponsor: Wenner-Gren Foundation for Anthropological Research; Grant sponsor: L.S.B. Leakey Foundation.

*Correspondence to: Patrick R. Hof, Kastor Neurobiology of Aging Laboratories, Mount Sinai School of Medicine, Box 1639, One Gustave L. Levy Place, New York, NY 10029. Fax: (212) 849-2510. E-mail: patrick.hof@mssm.edu

Received 27 June 2002; Accepted 4 October 2002
DOI 10.1002/ar.a.10015

area 4a (agranular, devoid of Betz cells), and area 4s (agranular, without Betz cells, but containing large cells in superior part of layer IV (von Bonin, 1949)), and a frontal ganglionic core, all of which are to some extent part of the original description of Brodmann's area 4. More recent studies have shown that the primary motor cortex can be divided into two different subareas, 4a (anterior) and 4p (posterior), which differ by their cytoarchitecture and distribution of various neurotransmitter binding sites (Geyer et al., 1996). Although it is now widely accepted that the caudal boundary of the primary motor cortex is characterized by the appearance of a granular layer IV (in area 3a), an increasing cellular density in supragranular layers, and a sharp division between white and grey matter, the rostral limit of the primary motor cortex remains more controversial (Smith, 1907; Bailey and von Bonin, 1951; Zilles, 1990; Geyer et al., 1996, 1999; White et al., 1997a, b). According to Brodmann's original definition of the primary motor cortex, based on the presence of Betz cells, the absence of these cells anteriorly was considered a critical landmark for the boundary between areas 4 and 6.

The recognition of Betz cells in Nissl preparations is itself problematic, because they share most of their morphologic features with other large pyramidal neurons in layer V (Walshe, 1942; Kaiserman-Abramof and Peters, 1972; Braak and Braak, 1976; Wise 1985). Therefore, cell body size cannot be reliably taken as the sole discriminative feature of Betz cells. In fact, Betz cells differ from other pyramidal cells by their dendritic morphology. In most pyramidal cells, with the exception of the apical shaft, dendritic arbors leave the cell body almost exclusively from basal angles and some of the largest cells have as many as six primary basal dendrites. Betz cells, however, have a higher number of primary dendritic shafts that leave the cell body asymmetrically at almost any point around the cell's basal surface (Scheibel and Scheibel, 1978; Meyer, 1987), as well as from the cell body itself (Braak and Braak, 1976). The apical dendrites and soma of Betz cells are oriented along a vertical axis, which may contribute to columnar processing in the primary motor cortex (Meyer, 1987). Also, Betz cell somata are heterogeneous in shape, and include pyramidal, triangular, and spindle-shaped cell bodies (Braak and Braak, 1976).

Betz cells are found either solitarily or in small groups of three to four cells, especially in the dorsal part of area 4 (Brodmann, 1909; von Bonin, 1949). They have been reported to occur preferentially in the lower half of layer V, thereby allowing for the distinction of two sublayers within layer V (layers Va and Vb (von Economo and Koskinas, 1925; Meyer, 1987)). The size of the Betz cell bodies has been reported to decrease continuously along a mediolateral gradient (von Bonin, 1949; Zilles, 1990). This size reduction appears to be related to motor somatotopy: the largest cells are found in the region of foot and leg representation, where efferent axons project the farthest along the corticospinal tract. The values reported in early studies for the total number of Betz cells in one human hemisphere range from 25,000 (Campbell, 1905), to 34,370 (Lassek, 1940; Lassek and Wheatley, 1945; Blinkov and Glezer, 1968), and up to 40,000 (Scheibel and Scheibel, 1978). Lassek (1940) demonstrated that the numerical distribution of Betz cells is related to somatotopy, with 75% of all Betz cells being in the leg area, 17.9% in the arm region, and 6.6% in the head area. However, his functional demarcation was not based on visible cytoarchitectural differences that could permit a precise definition of functional motor zones.

No recent studies have assessed Betz cell numbers, volumes, and distribution in normal human brains. The aim of this study was to estimate these parameters for Betz cells of the human primary motor cortex, in comparison to other layer Vb pyramidal neurons. In this study, we used modern stereologic techniques and Voronoi tessellation to obtain normative data about the cellular population of layer Vb of the human primary motor cortex, and to correlate microscopic morphologic architecture with macroscopic anatomy and functional results obtained by functional MRI (fMRI) (Yousry et al., 1997; Boroojerdi et al., 1999).

MATERIALS AND METHODS

Tissue Acquisition and Preparation

All brains used in this study were obtained from six deceased elderly individuals (five women and one man; 75–96 years old) with no record of neurologic or psychiatric disorder, who had been hospitalized in the Department of Geriatrics, University of Geneva, Switzerland. In particular, none of these cases demonstrated any sensorymotor deficits on admission to hospital and no such symptoms were recorded during their terminal illness. It must also be noted that while age-related alterations in the dendritic arborizations of Betz cells and of other pyramidal neurons have been reported in human and nonhuman primates (Scheibel et al., 1977; Nakamura et al., 1985; Tigges et al., 1992; Hof and Duan, 2001; Hof and Perl, 2002; Page et al., 2002), the number of neocortical pyramidal neurons does not decrease during normal aging (Hof et al., 1999; Bussière et al., in press). Moreover, the primary motor cortex is generally spared, even in late stages of Alzheimer's disease (Arnold et al., 1991). It is thus unlikely that the advanced age of the patients included in this study influenced the outcome of our analyses. The brain specimens were collected at autopsy within 12 hr of death and were fixed by immersion in 10% buffered formalin for up to 9 days. Only the left hemispheres were used. The precentral gyrus, central sulcus, and postcentral gyrus (to ensure that the entire extent of area 4 was available) were dissected out and separated into six or seven equally sized blocks, depending on the mediolateral length of the primary motor cortex for stereologic analyses (Fig. 1) (Perl et al., 2000). These tissue blocks were subsequently cryoprotected by immersion in graded sucrose solutions (up to 25%) and sectioned at 50 μm on a cryostat perpendicular to the axis of the central sulcus. All sections were kept in strict serial order. From each block a 1:20 series of sections was mounted on gelatin-coated slides, stained for Nissl substance with cresyl violet, and coverslipped with Entellan.

Stereologic Analyses

The volumes and numbers of Betz cells and neighboring pyramidal neurons were estimated using a computer-assisted image analysis system consisting of a Zeiss Axiophot 2 microscope equipped with a Zeiss MSP65 computer-controlled motorized stage, a Zeiss ZVS-47E video camera, a Macintosh G3 microcomputer, and NeuroZoom, a custom-designed morphometry and stereology software (Young et al., 1997; Nimchinsky et al., 2000).

One section per block was sampled in each case using a systematic-random design and cell numbers were esti-

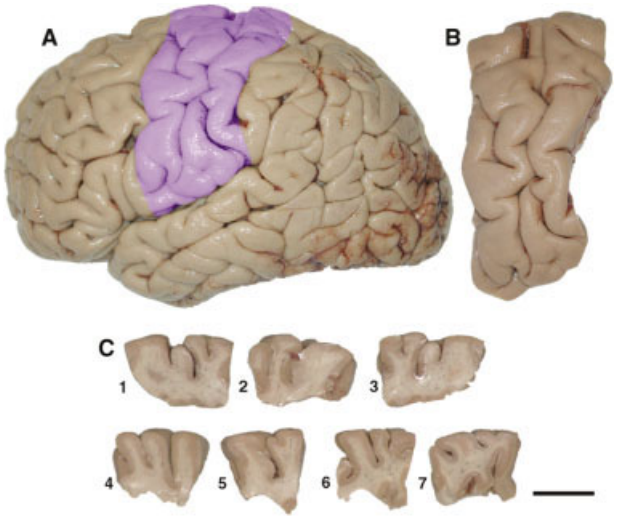

Fig. 1. Localization of the primary motor cortex and dissection methods. **A:** Area 4 is located in the depth of the central sulcus and on the anterior bank of the precentral gyrus. **B:** In each analyzed hemisphere, the central sulcus, precentral, and postcentral gyri (colored purple), were dissected out. **C:** Depending on the case, six or seven blocks were cut from the dissected cortical specimen. The blocks were prepared in equal size, and their total number varied according to individual differences in the extent of the motor cortex. Blocks were kept in a strict medial to lateral orientation for sectioning and staining. In C, block 1 is medial and block 7 is lateral, and the lateral face of each block is shown. Scale bar = 2 cm.

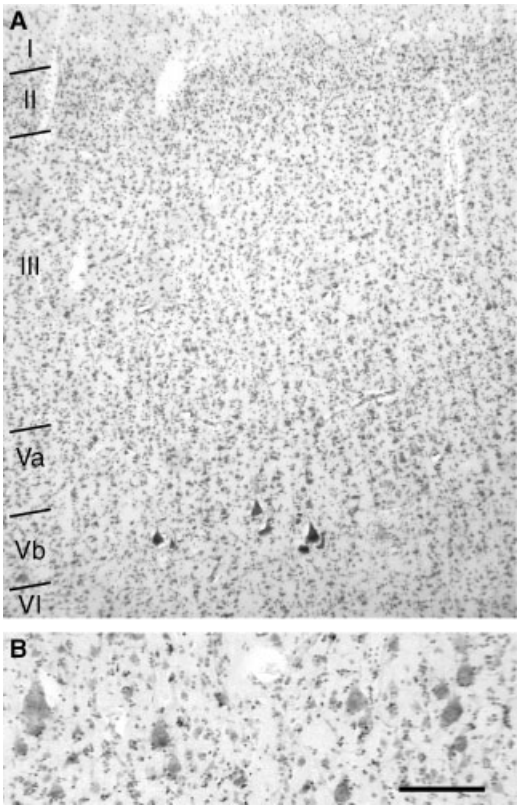

Fig. 2. **A:** Laminar organization of the primary motor cortex. **B:** Betz cells appear scattered throughout layer Vb, some of which form clusters. These photomicrographs were taken from sections located in blocks 3 and 4, in the region of the "hand-knob." Layer boundaries are indicated in panel B. Scale bar (on B) = (A) 200 μm, and (B) 100 μm.

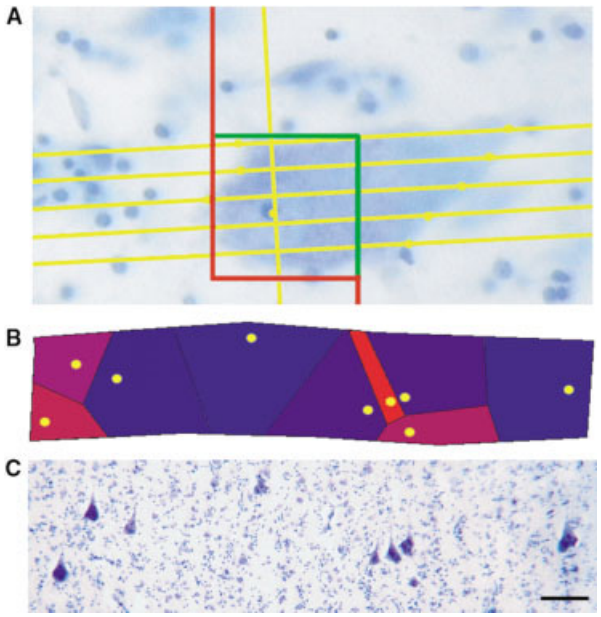

Fig. 3. **A:** Quantification of neuronal number and volume with the NeuroZoom software. A disector counting frame of 50 μm × 50 μm was used. Five rotator test lines can be seen crossing the Betz cell soma, with dots pointing to their intersections with the soma border. **B:** For analysis of Betz cell distribution, we generated high-magnification Voronoi tessellation maps. **C:** A view of the corresponding microscopic field. Betz cells are represented by yellow dots, and the size of the polygon drawn around them is inversely proportional to their individual packing density. The smallest polygons, color-coded in red, are zones wherein clustering occurs. Scale bar = (B and C) 100 μm.

mated using the optical fractionator (West et al., 1991). Betz cells are located preferentially in the lower half of layer V of area 4 (von Economo and Koskinas, 1925), effectively subdividing the relatively thin layer V (about 0.7 mm in our materials, compared to the 0.8–0.9 mm of von Economo and Koskinas [1925]), into two sublayers. Some authors have recognized subdivisions of layer V in area 4 (von Economo and Koskinas, 1925; Meyer, 1987). Layer Va is characterized by a dense population of large pyramidal neurons that have a rather homogeneous apparent distribution (Fig. 2). Layer Vb is conspicuous due to the presence of the giant Betz cells in addition to large pyramidal neurons. Betz cells are considerably larger than any other cell types in this layer. Also the apparent density of neurons is generally lower in layer Vb than in layer Va. Large pyramidal cells of any type are not present in layer VI, which allows a clear boundary to be defined between layer V and VI (Fig. 2). We did not consider Betz cells the main discriminating feature of the primary motor cortex, but rather one among many criteria. After defining the boundaries of layer Vb on the computer graphic display of each section, the NeuroZoom software placed within each laminar boundary a set of optical disector frames (50 μm × 50 μm) in a systematic-random fashion corresponding to 3% of the sampled area for Betz cells or adjacent pyramidal cells. Neurons were then analyzed in each stack of optical dissectors (each disector was 5 μm in

depth if a neuron corresponding cytomorphologically to a Betz cell was encountered (see below for criteria), and 2 μm for other pyramidal cells), according to stereologic principles. The thickness of these disector stacks, termed "multisectors" in the NeuroZoom software (Nimchinsky et al., 2000), was kept constant within each case and depended on the measured thickness of the sampled sections, which varied between 15 and 20 μm among cases. The shrinkage resulting from histological processing did not influence the estimates of total neuronal numbers as the optical fractionator does not depend on a calculation of the total volume of the region. Sampling of Betz cells and surrounding pyramidal cells was thus accomplished through the entirety of the section's thickness (except for a 2-μm guard zone on either side of the sections). Interneurons were not included in the analysis.

For the rotator analysis, which was combined with the optical fractionator (Fig. 3A), the vertical axis of the probe was a line running strictly superior-to-inferior with respect to the pial surface, as it was not possible to perform isotropic-uniform-random sections in the available materials. However, coronal sections and isotropic-uniform-random sections have been shown to yield comparable results (Schmitz et al., 1999). Furthermore, because of the orientation of the tissue in our preparations, not all neurons were necessarily cut along the same axis, thereby allowing for a certain degree of randomness in the sample. Only neurons whose nucleus was enclosed within the counting frame or in contact with its permitted edges were analyzed, and the nucleolus was consistently chosen as a reference landmark for the focal plane during fractionator and rotator analysis. During data acquisition, Betz cells were tentatively identified by a conspicuous nucleolus, a prominent rough endoplasmic reticulum, large lipofuscin deposits in the cell body, and a dendritic arbor leaving from the entire surface of the soma (Scheibel et al., 1977; Braak and Braak, 1979; Zilles, 1990). All analyses were performed using a 1.4 N.A. 40x Plan-NeoFluar Zeiss objective with a 1.4 N.A. auxiliary condenser lens and Koehler illumination to achieve optimal optical sectioning. Using this stereologic design, on average 372 Betz cells (2,229 total) and 224 non-Betz pyramidal neurons (1,344 total) were sampled and analyzed in each brain.

Statistical comparisons were made between blocks in order to determine whether differences in neuron number or cellular volume existed between different mediolateral locations along area 4, by use of a one-way analysis of variance (ANOVA) and post-hoc *t* tests. Blocks were numbered from 1 (most medial) to 6 or 7 (most lateral). Coefficients of error and coefficients of variation were also calculated (Schmitz, 1998; Schmitz and Hof, 2000). To assess the distribution of cellular volumes, we calculated the percentage of cells (without distinguishing between Betz and pyramidal cells) within volume bins for each case. The cumulative frequency of each volume bin was also calculated. Statistical differences between volume distributions based on these cumulative frequencies were assessed using the Kolmogorov-Smirnov test.

Analysis of Betz Cell Distribution

Betz cells from the same systematic-randomly sampled sections used for stereological analysis were mapped along the primary motor cortex using NeuroLucida software (MicroBrightfield Inc., Williston, VT). The boundaries of layer Vb of the primary motor cortex were drawn using 5× or 10× Fluar Zeiss objectives, and markers were placed on all visible Betz cells. These maps were then converted to polygon maps using Voronoi tessellation. With the VORON software (Duyckaerts and Godefroy, 2000), Voronoi tessellations estimate in two dimensions the degree to which particles are clustered, randomly distributed, or have regular arrangements. It tests only the distribution of particles—not their numbers or densities—in the entire region analyzed. This approach is based on a principle by which polygons are drawn around mapped points (in this case, Betz cells) according to a simple algorithm that bisects each tangent connecting a particle to each of its closest neighbors. The resulting polygon area is inversely proportional to the local cell packing density (Duyckaerts and Godefroy, 2000). A density mosaic is formed by these polygons, with the smallest polygons occurring where cells have a clustered distribution (Fig. 3B and C). The general coefficient of variation (GCV), local coefficient of variation (LCV), and coefficient of clustering were calculated. The GCV was calculated on the basis of all the polygon areas within a section. The LCV is the mean of the coefficient of variations of all of the individual polygons and their immediate neighbors. The coefficient of clustering represents the ratio GCV/LCV and reflects cells distribution. If the cells are randomly distributed, the LCV will tend to be equal to the GCV and the coefficient of clustering will be close to 1. In contrast, if the ratio GCV/LCV is high, cells represented by marked points are clustered (Duyckaerts and Godefroy, 2000). For each case the block in which the Betz cells were maximally clustered (i.e., where the coefficient of clustering was maximal) was identified. The total number of Betz cells in this block was estimated as a fraction of the total for the whole area 4 as determined by the optical fractionator. ANOVA and post-hoc pair-wise *t*-tests with Sidak and Bonferoni correction were used to assess differences in the coefficient of clustering among blocks in all of the cases.

To illustrate the distribution of cell volumes and clusters on the surface of a brain hemisphere, the amount of tissue lost between blocks during the initial sampling was considered for each case (<1 mm was lost per block), and an individual correction factor was calculated to estimate the actual length of the primary motor cortex. Regional maxima in cellular volume and clustering were then depicted on a digital image of the brain surface using Adobe Photoshop software. All photomicrographs were obtained using a Nikon CoolPix 990 digital camera mounted on a Zeiss Axiophot 2 photomicroscope, processed using Adobe Photoshop 5.5, and printed on a high-resolution Fujix Pictrography 3000 color printer. Only minor adjustments of contrast and brightness were performed, which in no case altered the appearance of the original materials.

RESULTS

Histologic Criteria

To analyze the Betz cell number and volume in layer Vb of the primary motor cortex (Fig. 2) adequately, a reliable set of identifying criteria had to be defined. Based on previous histological descriptions of Betz cells (Campbell, 1905; Brodmann, 1909; Walshe, 1942; Scheibel and Scheibel, 1978; Braak and Braak, 1979), we considered large pyramidal neurons displaying a conspicuous nucleolus, a prominent rough endoplasmic reticulum, large lipofuscin deposits in the cell body, and dendritic branches leaving from the entire circumference of the soma to be Betz cells

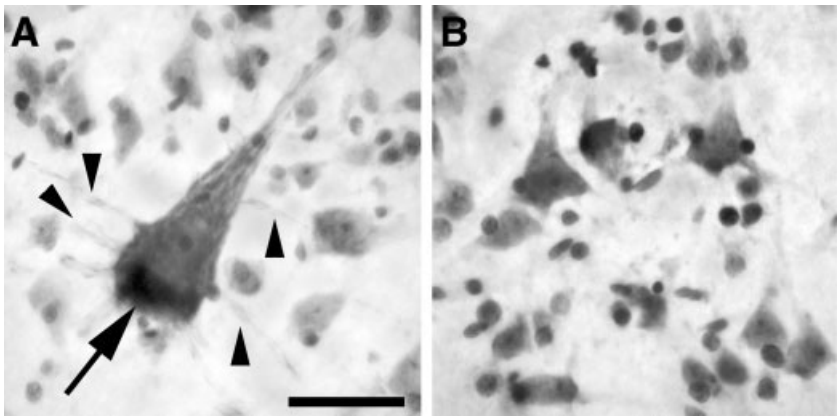

Fig. 4. High-magnification photomicrographs comparing the histologic characteristics of (**A**) a Betz cell to (**B**) neighboring pyramidal cells. Note the larger size, conspicuous nucleolus, abundant rough endoplasmic reticulum, perisomatic dendrites (in addition to the basal dendrites (arrowheads)), and lipofuscin accumulation (arrow). These were the cytomorphologic criteria used to identify Betz cells during the analysis. Scale bar = 80 μm.

(Figs. 4A and 5). In contrast, adjacent non-Betz pyramidal cells were recognized precisely by the lack of all of these characteristic morphological features (Fig. 4B). Betz cells themselves were variable in shape. Betz cells that were located deeper in the central sulcus next to the boundary with area 3a were more triangular or rounder than the ones located near the anterior boundary of primary motor cortex, which had a fusiform shape (Fig. 5).

Cytoarchitectural criteria were used to outline the boundaries of the primary motor cortex. The posterior limit of the primary motor cortex (between Brodmann's areas 3a and 4) was more difficult to establish with precision, and in this study was placed where layer IV, which is clearly identified in area 3a, disappeared, and where the limit between the white and gray matter became blurred (White et al., 1997b). The anterior boundary of the primary motor cortex (between Brodmann's areas 4 and 6) was placed in the middle of a transitional zone where large pyramidal neurons begin to appear in layer III.

Stereologic Assessment of Cell Numbers and Volumes

The total number of Betz and pyramidal cells in layer Vb of the left primary motor cortex was estimated using the optical fractionator (Table 1). The number of Betz cells ranged among the six cases from 96,220 to 165,920 cells, with a mean of 125,290 cells. In comparison, the average number of non-Betz pyramidal cells in layer Vb was 1,026,630 cells, with a range of 471,240–1,673,740 cells. The total number of pyramidal neurons in layer Vb was on average 1,151,920 cells, with values ranging from 567,460 to 1,973,700 cells. The percentage of Betz cells in comparison to the total number of pyramidal neurons was determined: on average, the Betz cell population represents 12.2% (range: 5.1–17%; Table 1) of the pyramidal neurons in layer Vb. The great amount of variability in the numbers of pyramidal neuron subtypes in layer V could not be explained by sex or age differences.

The volumes of Betz cells were estimated with the rotator (Fig. 2A; Table 1). The mean Betz cell volume was 86,685 μm^3 (range among the six cases: 66,010–113,146 μm^3). The average non-Betz pyramidal cell volume was 4,274 μm^3 (range for all cases: 3,606–4,826 μm^3). The overall mean volume of all pyramidal neurons in layer Vb was 90,959 μm^3, ranging from 70,835 to 117,417 μm^3 depending on the case. To compare the cellular volumes of Betz cells and pyramidal neurons, we calculated the ratio of the volumes of Betz cells to pyramidal cells (Table 1). Betz cell volumes were larger than the volumes of pyramidal cells by a factor of 20.4 ($P < 0.001$), supporting a clear distinction between these cellular populations based on somatic volume.

We expressed all cellular volumes (without categorical distinction) as a percentage of the total volume range. The distribution of the cellular volumes was clearly bimodal, with one peak at 3,000–4,000 μm^3, and another peak at 50,000–100,000 μm^3 ($P < 0.001$). A distinct volumetric cut-off was identified that differentiates pyramidal cells from Betz cells at 20,000 μm^3 (Fig. 6A). To estimate the small amount of overlap that may exist between these two cellular populations, we searched for the largest volume of a cell that we considered to be a non-Betz pyramidal cell (18,501 μm^3), and the smallest volume of a cell that we considered to be a Betz cell (10,905 μm^3; the next smallest value for Betz cells was 20,513 μm^3), according to our histologic criteria. We then calculated the percentage of cellular volumes found at 15,000–30,000 μm^3, without distinguishing between Betz cells and pyramidal non-Betz cells. We observed that 3.8% of all cellular volumes occupied this range. Making a categorical distinction (according to our criteria) between Betz and pyramidal cells, we found that 2.9% of pyramidal cells and 5.7% of Betz cells, respectively, fell within the range of 10,000 and 30,000 μm^3. These data show that there is minimal overlap between the volumes of these two different cell subtypes, and that where there is overlap the range is limited. To characterize further the distribution of the volumes of the two cell populations, we plotted the cumulative percentage of the volumes against the cell volumes. The resulting curves show that the cellular volumes increase sharply and in a parallel fashion at the two extremes of the volume ranges, confirming the presence of two distinct cellular types, which can be distinguished by their volumes based on these quantitative data ($P < 0.001$; Fig. 6B).

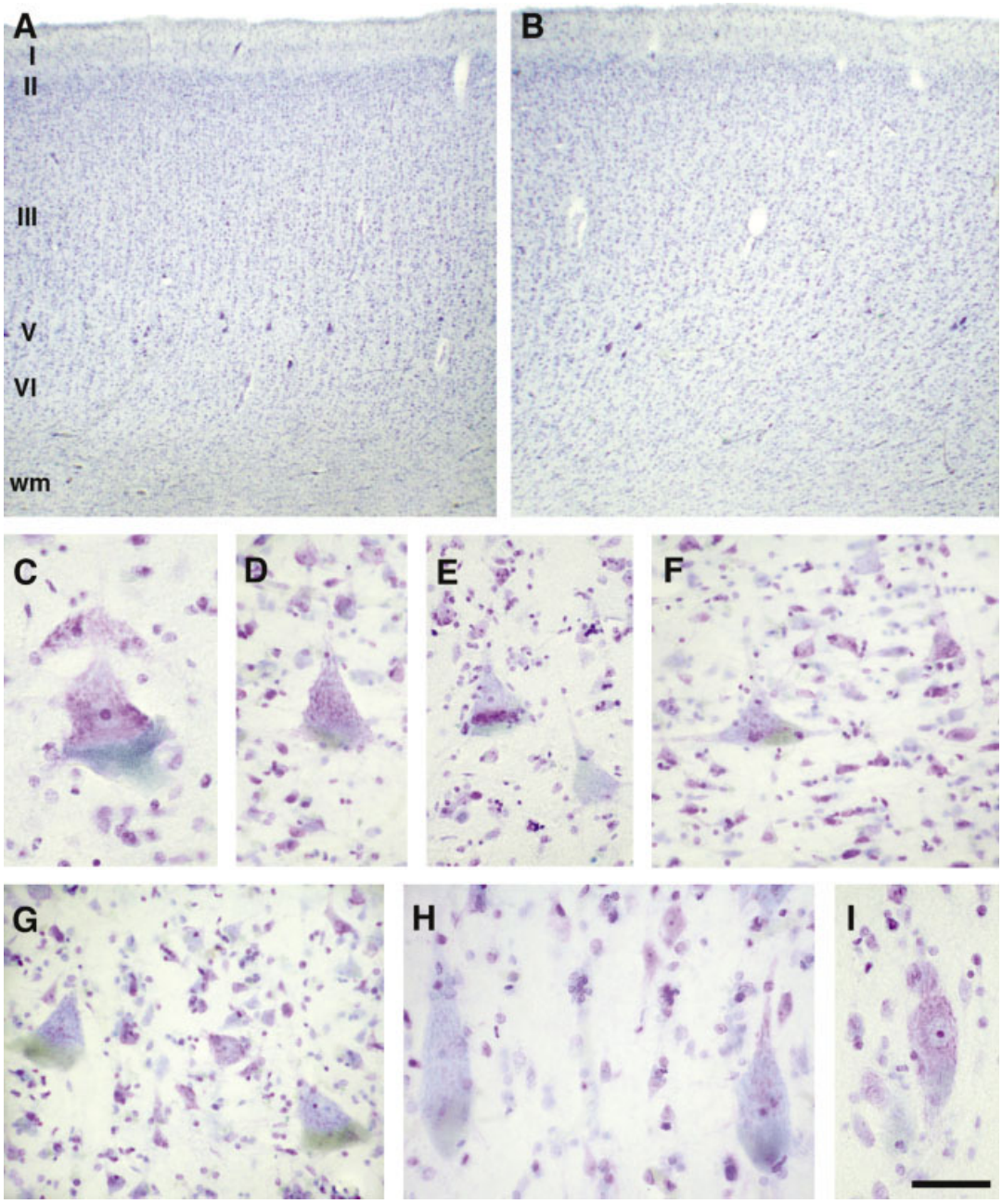

Fig. 5. Depending on their location in the primary motor cortex, the Betz cells exhibited morphological variability. Toward the depth of (**A**) the central sulcus, and in (**C–F**) the vicinity of the border of area 3a, rounder or squatter Betz cells were observed. In (**G**) the "hand-knob" region they were nearly triangular, whereas at (B) the rostral boundary of the primary motor cortex near the border to area 6, (**H** and **I**) the Betz cells adopted a more fusiform shape. Scale bar (on I) = (A and B) 300 μm, and (C–I) 50 μm.

For each case, Betz and pyramidal cell volume differences were analyzed according to block number, thus reflecting their mediolateral location (Fig. 7A). For all six cases, the Betz cell volumes decreased from block number 1 (medial) to block number 6 (lateral). We calculated the average volume per block across all of the cases (Fig. 8A), and block number 2 consistently contained Betz cells with the largest volumes ($P < 0.05$). This confirms the observation of von Bonin (1949) that Betz cell volume follows a mediolateral gradient along the primary motor cortex. Non-Betz pyramidal cell volumes expressed per case and as a mean per block were homogeneous throughout the primary motor cortex (Figs. 7B and 8B). The fact that the largest Betz cells were located in the medial portion of the primary motor cortex (Figs. 8A and 9H) corroborates the observation that the size of the Betz cells is larger in the areas representing the foot and leg (Lassek, 1940; Zilles, 1990).

TABLE 1. Betz cell and pyramidal cell numbers and volumes

Cases	Betz cells	CE	Pyramidal cells	CE	Total	CE	Betz %
Neuronal numbers							
A	134,300	0.05	1,189,320	0.10	1,323,620	0.04	10.1
B	144,840	0.05	953,700	0.11	1,098,540	0.04	13.2
C	96,220	0.06	471,240	0.15	567,460	0.06	17.0
D	110,500	0.06	729,300	0.12	839,800	0.05	13.2
E	99,960	0.06	1,873,740	0.13	1,973,700	0.05	5.1
F	165,920	0.05	942,480	0.11	1,108,400	0.04	15.0
Mean	125,290.0		1,026,630.0		1,151,920.0		12.2
SD	27,639.1		480,276.3		479,282.6		4.2
CV	0.22		0.47		0.42		

Cases	Betz cells	Pyramidal cells	Betz/pyramidal cells
Neuronal volumes			
A	110,146.0	4,514.1	24.4
B	79,112.2	3,936.2	20.1
C	72,845.5	3,606.1	20.2
D	66,009.6	4,826.1	13.7
E	113,125.2	4,292.1	26.4
F	78,876.7	4,468.9	17.7
Mean	86,685.9	4,274.0	20.4
SD	19,934.0	438.3	4.6
CV	0.23	0.10	0.23

The raw data from the stereologic analysis of each case are shown, as well as the mean, standard deviations (SD), coefficients of variation (CV), and coefficients of error (CE). The Betz percentage represents the proportion of Betz cells from the total number of layer Vb pyramidal neurons in the primary motor cortex (top). The ratio of Betz cell volume to pyramidal cell volume was calculated to compare the cellular volumes of these two distinct populations of neurons (bottom).

Tessellation Maps and Coefficient of Clustering

The distribution of local Betz cell densities was assessed using Voronoi tessellation (Duyckaerts and Godefroy, 2000). The resulting distribution patterns were similar in all cases, showing high Betz cell clustering in the medial part of the primary motor cortex, and a progressive decrease in density toward the Sylvian fissure (Fig. 9A–G). To confirm this, we analyzed the coefficient of clustering of Betz cells in each case (Fig. 10A). In five of the six cases this coefficient was maximal for block numbers 3 or 4. In one case (case E), the maximum of the coefficient of clustering was located in block number 2. However, when all of the cases were analyzed together with ANOVA, the coefficient of clustering in block 4 was significantly greater than that in other blocks ($P < 0.05$; Fig. 10B). Due to interindividual variability in motor cortex length, the number of blocks was not equal in all of the cases, which may have biased the results when expressed per block number. Tessellation maps and coefficient of clustering statistics of Betz cells were produced from all of the slides from one reference case (case F). The results were comparable to the analysis performed in the other cases in which only one slide per block was analyzed, with a maximal coefficient of clustering located at approximately two-thirds of the length of the primary motor cortex laterally from the interhemispheric fissure. To illustrate the localization of this area of maximal Betz cell clustering, we estimated its position on the cortical surface of each case separately. This area is located roughly at the junction of the superior and medial frontal gyri with the precentral gyrus (summarized in Fig. 9H and I), corresponding generally to the previously described "hand-knob" region (Yousry et al., 1997; Boroojerdi et al., 1999; Takahashi et al., 2002). Interestingly, this analysis also demonstrates that while the area of maximal clustering occurs in blocks 3 and 4, the region of area 4 where Betz cells are most numerous corresponds to the representation of the leg (blocks 1 and 2), in agreement with Lassek's earlier findings (Lassek, 1939, 1940, 1954) (Fig. 9). Other pyramidal cells showed a uniform spatial distribution pattern throughout the entire primary motor cortex.

DISCUSSION

Overview of Quantitative Findings

The present study demonstrates that the Betz cells of the human primary motor cortex represent a heterogeneous neuronal population in terms of size, shape, volume, and distribution. The use of a rigorous stereological approach to estimate volumes and total numbers of all pyramidal neurons in layer Vb also revealed notable differences in comparison to results from earlier studies of Betz cells (Campbell, 1905; Lassek, 1939). This study demonstrates that Betz cells have different distribution patterns within the human primary motor cortex in terms of their shape, volume, and clustering. The observed differences in Betz cell shape in the anterior and posterior part of the primary motor cortex may be related to two distinct subareas in primary motor cortex (Geyer et al., 1996). The distribution of the volumes of Betz and other pyramidal cells follows a bimodal distribution with two maxima, delineating two different neuronal populations with a clear cut-off at values around 20,000 μm^3 (the overlap of these two separate populations representing approximately 3.8% of the total of the volumes analyzed). More-

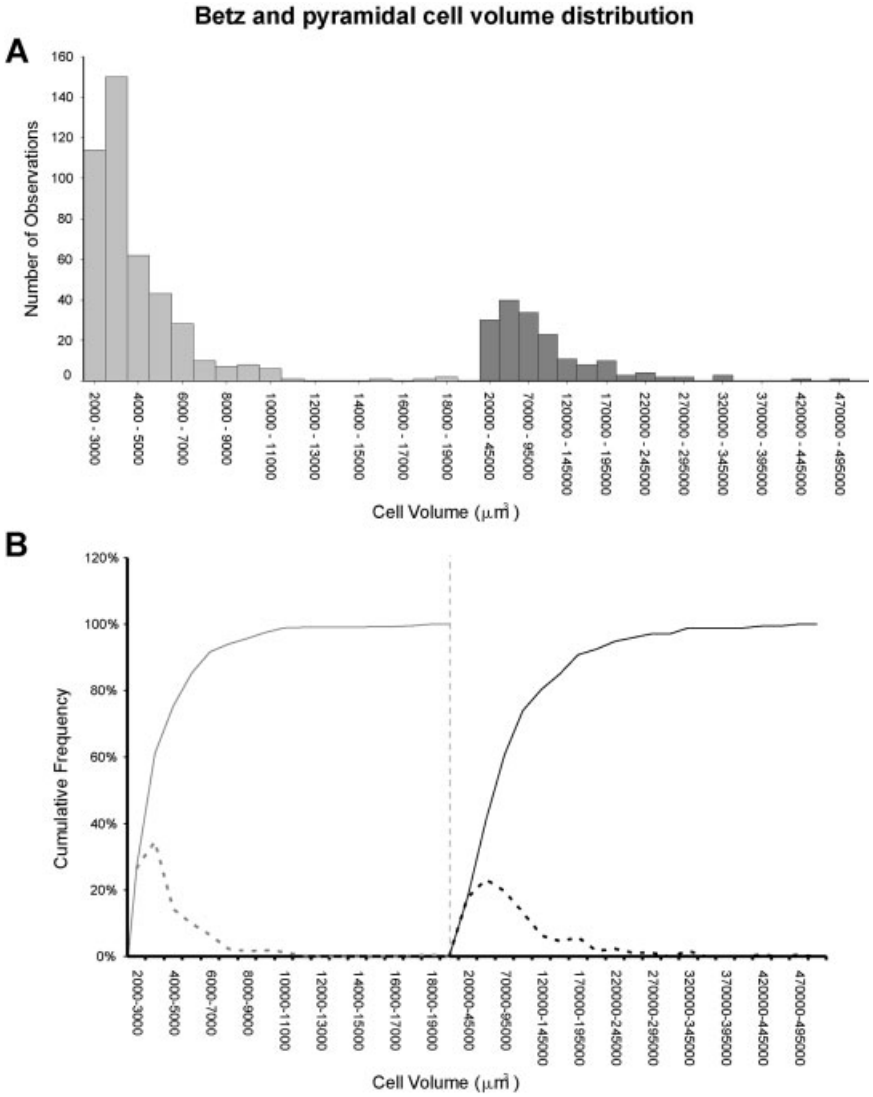

Fig. 6. Betz cell and layer Vb pyramidal cell volume distributions. Histograms of cell volumes expressed as (**A**) the total number of cells observed within volume bins, and (**B**) as a percent and cumulative frequency of the distribution of volumes by subtype. Pyramidal cell volumes appear on the left and Betz cell volumes on the right. A: The volume distribution is strongly bimodal, with maximal pyramidal cell volumes of 3,000–4,000 μm^3 and maximal Betz cell volumes of 50,000–100,000 μm^3. The cut-off point for distinguishing Betz cell from pyramidal cell volume appears clearly around 20,000 μm^3. B: The cumulative frequency clearly shows the difference between the two populations. Note that, since Betz cells volumes are distributed over a much greater range than pyramidal cells, the *x*-axis scales differ for Betz and pyramidal cells.

over, Betz cell volumes follow a mediolateral gradient along area 4, as first suggested by Brodmann (1909) and von Bonin (1949), which is likely to be correlated with the functional motor representation of the hind limb. In contrast, the volume of other pyramidal cells in layer Vb is homogeneous, and does not differ along the mediolateral axis of the region. Analyses of spatial distribution indicated that Betz cells are organized as a specialized group of neurons forming clusters in layer V, and that their distribution along the human primary motor cortex is not homogeneous. Using Voronoi tessellations we demonstrated that Betz cells form clusters with a maximal clustering zone situated midway between the interhemispheric and Sylvian fissures (25,380 μm on average) in the region of the "hand-knob." Interestingly, if we consider the total number of Betz cells in the block showing the densest clustering, we found that on average 6,800 of them occur at this location (about 5.5% of all Betz cells), which is likely to correlate with the functional motor representation of the hand. This variability in Betz cell shape and distribution may provide new clues for further exploration of the relationships between functional anatomical zones and cytomorphologic characteristics of the primary motor cortex.

Boundaries of Human Primary Motor Cortex

In contrast to Brodmann's early descriptions, it has been widely recognized that the gross morphology of the

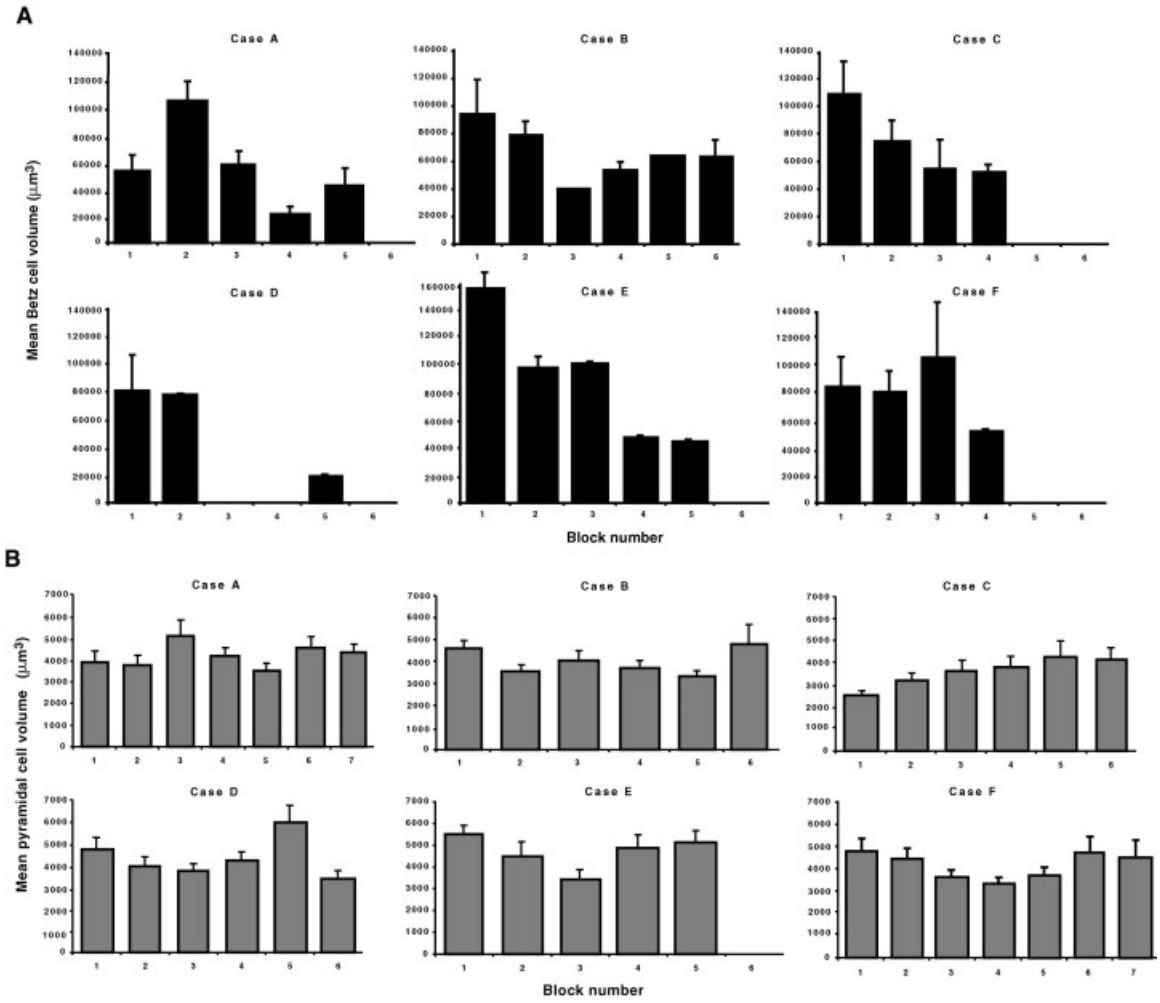

Fig. 7. Betz cell and pyramidal cell volumes expressed as a mean in each block, for each case separately. (**A**) Betz cell volumes are more variable along area 4, in contrast to (**B**) pyramidal cell volumes, which remain relatively comparable throughout the whole region. Missing values in panel A mean that no volume data were available from these blocks. Generally, Betz cells were very rarely observed in block 7.

cortical sulci and gyri does not correspond precisely to distinct functional areas (Rademacher et al., 1993; Geyer et al., 1996; White et al., 1997a, b; Rademacher et al., 2001), even if some evidence exists that certain sulci demarcate specific cortical areas (Vogt, 1910; Sanides, 1962, 1972; Welker and Campos, 1963; Zilles, 1990). Thus, the precentral gyrus and the depth of the anterior bank of the central sulcus cannot be used as reliable topographical criteria to precisely localize the primary motor cortex. It is generally accepted that Brodmann's area 4 represents the human primary motor cortex, or at least a major part of it. Brodmann's interpretation of area 4 as representing the human primary motor cortex (Brodmann, 1903, 1905, 1906, 1909) has led to misinterpretations, in part because of his schematic drawings, which provide no information about interindividual variability in the shape and cytoarchitecture of the brain (Filimonoff, 1932; Rademacher et al., 1993; Geyer et al., 1996, 1999; Zilles et al., 1997; Schleicher et al., 2000; Amunts et al., 2000). Misinterpretations also arose because of area 4's extension onto the convexity of the precentral gyrus. A recent study showed that area 4 itself includes two distinct zones (areas 4a [anterior] and 4p [posterior]) that differ quantitatively in cellular density and distribution of neurotransmitter binding sites, and exhibit separate functional patterns depending on the roughness or subtlety of the movements of the hand and digits, as demonstrated by positron emission tomography analyses (Geyer et al., 1996). This separation of the primary motor cortex into anterior and posterior zones based on cytomorphological and biochemical differences could be related to our observation of two different distinctive Betz cell shapes, with one group located in the depth of the central sulcus next to area 3a being rounder than the group located more rostrally at the junction with area 6.

Therefore, in view of the complexity of the definition of architectural and functional limits for the human primary motor cortex and, in extenso, of area 4, we decided to keep the definition of Brodmann's area 4 lamination patterns as a reliable delineation of the caudal boundary of primary

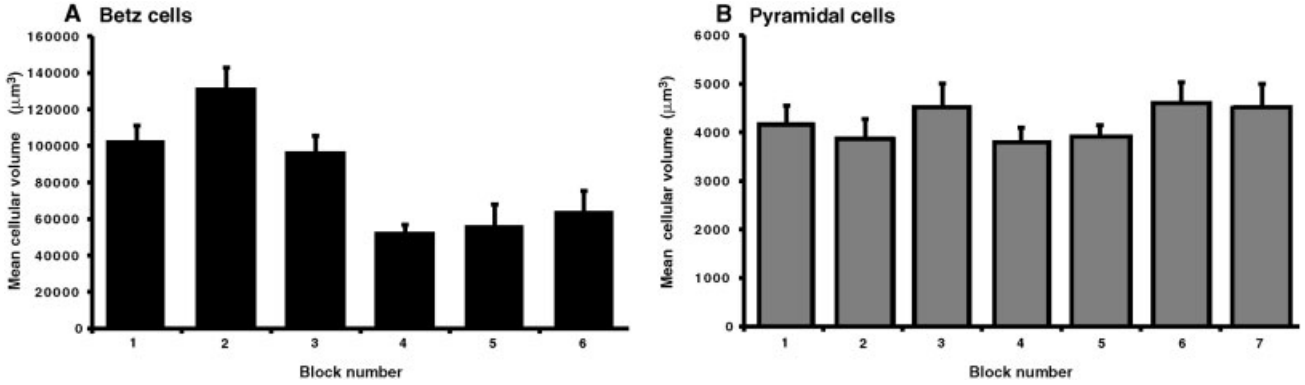

Fig. 8. Betz cell and pyramidal cell volumes expressed as a mean per block across all of the cases. **A:** Betz cell volumes are higher in block 2 than in the other blocks ($P < 0.05$). **B:** Pyramidal cell volumes do not differ significantly among blocks.

motor cortex, but we modified to some extent the definition of its rostral limit. This is important because it has been pointed out by many authors that Betz cells alone cannot be taken as a discriminating criteria for the rostral limit of area 4 (Wise, 1985; Zilles, 1990; White et al., 1997a; Geyer et al., 2000). In fact, their distribution may spread out on the anterior part of the precentral gyrus, in the caudal part of area 6.

Characteristics of Betz Cells vs. Layer V Pyramidal Cells

From the very first description of giant pyramidal cells by Betz (1874) to more recent studies, there has never been a clear morphologic distinction between Betz cells and their neighboring pyramidal neurons in layer Vb of the primary motor cortex. As their name implies, the giant pyramidal cells of Betz were categorized initially by their size, ranging from as small as 30 μm × 10 μm to as large as 120 μm × 60 μm (Betz, 1874; Lewis, 1878; Lewis and Clarke, 1878; Hammarberg, 1895; Brodmann, 1909; von Economo and Koskinas, 1925; Conel, 1941; Kaplan, 1952; Glezer, 1959; Blinkov and Glezer, 1968). These discrepancies explain attempts to find specific morphologic features that distinguish Betz cells (Walshe, 1942; Scheibel and Scheibel, 1978), the pigmentoarchitectonic analyses performed by Braak and Braak (1976), and the characterization of inclusion bodies among the lipofuscin deposits in aging Betz cells (Tigges, 1992), so as to be able to distinguish them from the other pyramidal cells in layer V. In view of the lack of definite criteria by which to discriminate Betz cells from other pyramidal neurons in layer V, we had to consider for the present study a constellation of cytomorphologic characteristics that permitted us to differentiate these two subpopulations of neurons, without considering their size as a criterion (see Results). Our results showed that the Betz cells, as we defined them, were about 20 times larger than the other pyramidal cells. Nevertheless, even if a categorical overlap in Betz and pyramidal cells size is unavoidable, the percentage of Betz cell and pyramidal cell volume distribution in layer Vb clearly demonstrated a bimodal distribution of the cellular volumes in layer Vb of the primary motor cortex, thereby implying that two different populations of neurons coexist and that one of their distinguishing features is indeed their volume.

With respect to the total number of Betz cells per hemisphere, the values reported by Campbell (1905), Lassek (1940), and Lassek and Wheatley (1945) represent underestimates by a factor of 3.6 in comparison to our results. These considerable discrepancies can be explained by the differences in the techniques used. Stereological analysis yields more accurate and unbiased estimates of neuronal counts compared to other quantification techniques (Howard and Reed, 1998). Our estimates reveal that about one-tenth of all pyramidal cells in layer Vb of the primary motor cortex are Betz cells.

Betz Cell Distribution Patterns and Functional Anatomy

Betz cells distribution can be considered according to two different characteristics: volume, and degree of clustering. A functional correlation between Betz cell volumes and the length of their projections was first made by Lassek (1939, 1940, 1954). Our results confirm that Betz cell volume is proportional to axonal projection length, as those located within the cortical domain corresponding to the motor representation of the leg and foot have the largest soma volumes. According to our findings, there does not appear to be another interpretation for these size differences.

Betz (1874), Lewis (1878), and Campbell (1905) noted that Betz cells are found in small clusters, heterogeneously scattered along layer V. A functional link for these clusters has not been discussed. We demonstrated that these clusters follow a specific distribution along the cortical motor strip. The classical motor representation of the "homunculus" (Penfield and Rasmussen, 1950), and more recent functional studies using modern techniques, such as fMRI, have pointed to the need for a microstructural basis for functional anatomical studies (White et al., 1997a, b; Geyer et al., 1999, 2000; Rademacher et al., 2001; Takahashi et al., 2002). Evidence of cytoarchitectonic differences in the cortical organization of the so-called "hand-knob," which is located on average about 23 mm from the midline, posterior to the junction of the superior frontal sulcus with the precentral sulcus, and 19 mm from the lateral surface (Yousri et al., 1997; Boroojerdi et al., 1999; Pizzella et al., 1999), has never been clearly established (White et al., 1997a,b). Our data show a maximal clustering zone located approximately midway

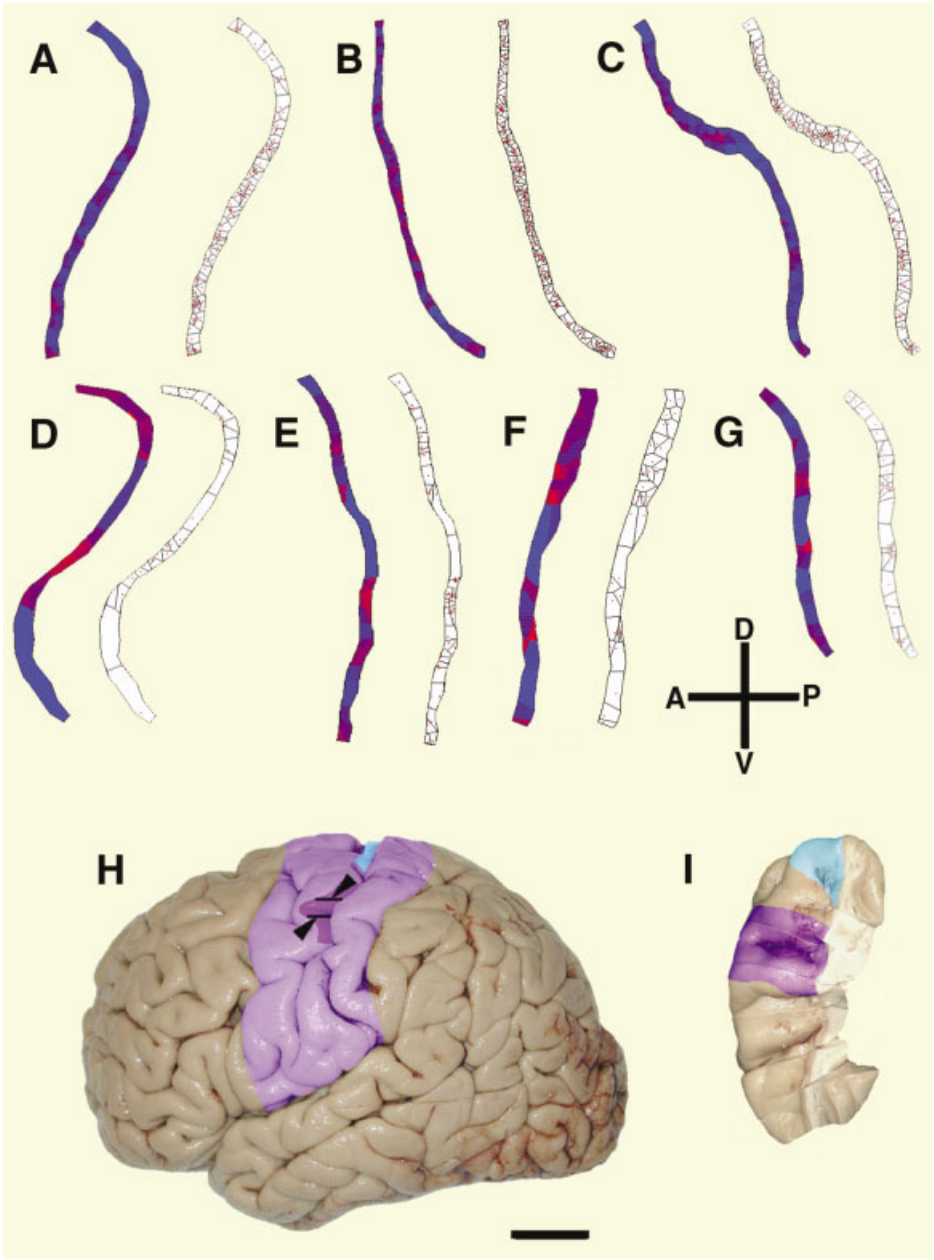

Fig. 9. **A–G:** Voronoi tessellation maps of layer Vb showing the analysis of the cellular density and clustering of Betz cells in case F. This example runs from block 1 (medial, A) to block 7 (lateral, G). On the color-coded maps, the smallest polygons (i.e., the regions of highest packing density) appear in red, while blue corresponds to the largest polygons (i.e., the regions with low packing density). The uncolored maps show the polygons drawn around the Betz cells, which are represented as red dots. In this analysis, the Betz cells appear to form clusters along the whole extent of layer Vb of area 4, as represented by the red polygons, with a maximal degree of clustering in blocks 3–5. All maps are shown to scale and are oriented in the same manner (G; the length of dorsal–ventral (D–V) or anterior–posterior (A–P) directions of the orientation key is approximately 5 mm and applies to A–G). **H:** The topographic distribution of Betz cell maximal volume and clustering on the primary motor cortex is shown on the same hemisphere as in Figure 1, with the dissected zone highlighted in purple. The zone with the largest Betz cells corresponding to the leg and foot representation appears in light blue. **I:** The zone of maximal Betz cell clustering across all of the cases is shown in dark purple and is also mapped onto a sulcal view of area 4. The localization of the tissue block with the maximal coefficient of clustering block in this case is shown (arrowheads and bars). Scale bar = (H and I) 2 cm.

from the midline and Sylvian fissure, which when illustrated on the cortical surface defines a zone that includes the "hand-knob" in its range. There is no overlap between the zones of maximal volume and maximal clustering of Betz cells, suggesting the presence of different, independent modes (shape, size, and clustering) of functional organization in layer V of the primary motor cortex. Thus, this zone of maximal clustering (containing approximately

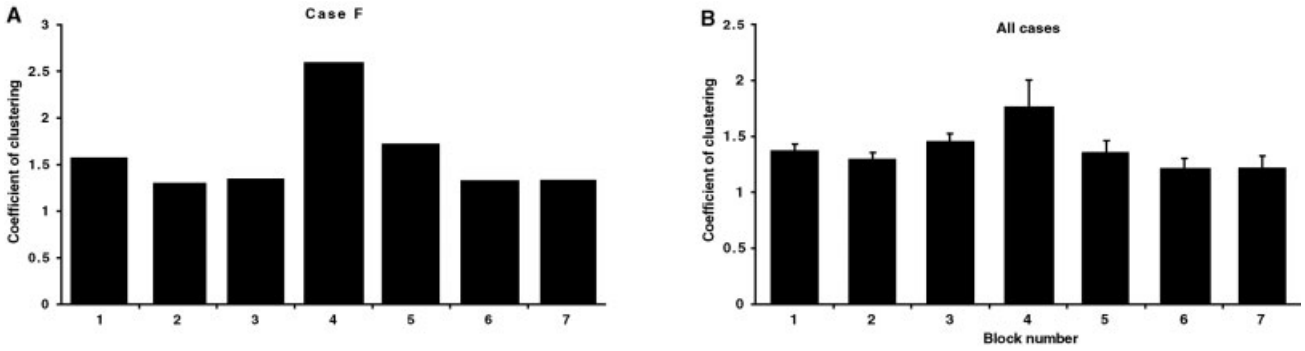

Fig. 10. **A:** The coefficient of clustering of Betz cells in case F reveals that the maximal clustering zone corresponds to block 4 (see also Fig. 9H). **B:** The mean coefficient of clustering of Betz cells across all of the cases was calculated from individual measures, and the values of mean clustering per block reveal that the zone of maximal Betz cell clustering is generally located in block number 4 ($P < 0.05$).

6,800 Betz cells) is likely related to the fine movements of the hand and wrist. Several factors, such as interindividual and sex differences in brain shape and primary motor cortex size, as well as postmortem tissue shrinkage, must be taken into consideration to assess the precise localization of this zone (Pakkenberg and Gundersen, 1997; Zilles et al., 1997; Amunts et al., 2000). Also, the lack of antemortem functional studies does not allow us to match precisely this zone of maximal clustering with a functional area. Nonetheless, the present observations suggest that these different patterns of clustering follow an organized distribution along the human primary motor cortex, and that they are highly correlated in each of our cases with the cortical region known to contain the motor representation of the hand (Yousry et al., 1997; Boroojerdi et al., 1999; Pizzella et al., 1999; Takahashi et al., 2002). Conversely, pyramidal cells in layer V do not show local patterns of distribution, but form a rather homogeneous population, corroborating previous observations (Campbell, 1905; Brodmann, 1909; Lassek, 1940).

While Betz cells exhibit a striking spatial distribution pattern that can be linked to general functional interpretations, their precise role has been poorly studied and remains undetermined. Available evidence suggests that Betz cells induce a fast release of antigravity extensor tone and flexor facilitation in select muscle groups before the onset of a specific motor command, and restore the extensor tone immediately thereafter (Lundberg and Voorhoeve, 1962; Evarts, 1965, 1967; Takahashi, 1965; Preston et al., 1967; Hore and Porter, 1972). It is possible that their particular distribution in different subdomains of area 4, and their extensive dendritic arborization enable these neurons to pool information about a motor program and to prepare the relevant spinal motoneurons prior to the onset of a given motor command. Our spatial distribution analysis demonstrates that the vast majority of Betz cells is located in the leg area, in agreement with Lassek's original observation. The fact that Betz cells are most numerous in the leg, even though the arm, hand, and face have a relatively larger cortical representation than the leg (Lassek, 1939, 1940, 1954), supports the notion that they play a major role in the control of antigravity muscles in humans. Similarly, our finding that about 5.5% of all Betz cells are maximally clustered in the hand area indicates that they are in a position to influence the control of fine digit, hand, and wrist movements that are uniquely developed in anthropoid primates.

Betz Cells, Neurodegenerative Diseases, and Normal Brain Aging

It is unclear how severely Betz cells are affected in neurodegenerative diseases such as amyotrophic lateral sclerosis. The reported degeneration of the dendritic arborizations, changes in synapses, and loss of Betz cells in amyotrophic lateral sclerosis and other degenerative illnesses involving the primary motor cortex suggest a participation of this neuronal subpopulation in the process of the disease (Hammer et al., 1979; Udaka et al., 1986; Kiernan and Hudson, 1991; Murayama et al., 1992; Nimchinsky et al., 1992; Nihei et al., 1993; Sasaki and Murayama, 1994; Pamphlett et al., 1995; Fujita et al., 1999; Sasaki and Iwata, 1999; Tsuchiya et al., 2000, 2002; Hof and Perl, 2002). The hypothesis that spinal motoneuronal degeneration is secondary to cortical transynaptic degeneration (Eisen et al., 1992), even if widely criticized (Pamphlett et al., 1995), has refocused attention on the possible involvement of the primary motor cortex in lower motoneuron disease. Many authors have attempted to establish a relation between neuronal loss and shrinkage in the spinal cord and in large motoneurons in the primary motor cortex (Marie, 1928; Davison, 1941; Lawyer and Netsky, 1953; Kiernan and Hudson, 1991; Nihei et al., 1993; Pamphlett et al., 1995) by comparing neuronal size between pathologic and control cases and quantifying the total number of motoneurons in different cortical and spinal regions. These studies have limitations in that the neuronal distribution patterns in layer V of the primary motor cortex were considered random, and estimates of neuronal sizes were expressed as diameters (i.e., in a two-dimensional plane based on variable criteria). In contrast, the Betz cells were shown in our study to be diverse in somatic volume and spatial organization. Gredal et al. (2000) used stereological methods to estimate total neuronal number in neocortex and in the motor cortex with the optical disector, and estimated regional volumes using the Cavalieri principle. However, different subpopulations of neurons, such as the Betz cells, were not analyzed separately. In this regard, it would be informative to evaluate

Betz cell loss and shrinkage in degenerative diseases affecting motoneurons using standardized and rigorous quantitative methods in postmortem human brains. Indeed, a limitation to this approach is that it requires access to whole specimens that can be adequately prepared and sampled according to stereologic principles (Perl et al., 2000).

In normal aging brains, Betz cells have been reported to have reduced dendritic spines and to swell; these age-related changes have been considered a possible correlate of the slowing of motor performance and agility, as well as increased stiffness during the lifespan (Scheibel et al., 1977), as Betz cells are preferentially involved in regulating the tone of antigravity muscles (Lundberg and Voorhoeve, 1962; Evarts, 1965, 1967; Takahashi, 1965; Preston et al., 1967; Hore and Porter, 1972). A decrease in the size of Betz cell somata has been reported in aged rhesus monkeys, along with a progressive appearance of highly specific, age-related inclusion bodies scattered within their lipofuscin deposits (Tigges, 1992; Tigges et al., 1992). However, these data were not obtained using a stereologic approach, and contradict previous observations of swelling of Betz cells during aging in humans (Scheibel et al., 1977).

The fact that Betz cells may be affected during aging is important considering the fact that our study had access only to the brains of elderly patients. It must be emphasized that although none of our cases suffered from motor deficits, it remains possible that a certain degree of dendritic or somatic attrition had occurred (Scheibel et al., 1977; Nakamura et al., 1985), which may have affected our estimates of Betz cell volumes. However, this is unlikely to have significantly affected this parameter, as the range of volumes that we obtained is well within that reported by previous authors in younger cases (about 25,000–113,000 μm^3 (Kaplan, 1952; Glezer, 1959; Blinkov and Glezer, 1968)). Furthermore, the aging process most likely did not influence the total numbers of Betz cells (and of other pyramidal cells), because stereologic estimates of total neuronal numbers have failed to reveal cell loss in normal brain aging (Hof et al., 1999; Bussière et al., in press). Of note, the primary motor cortex is generally spared in Alzheimer's disease at least until the very late stages of the dementia (Arnold et al., 1991), and pathological changes in large neurons are observed only in atypical cases with prominent motor symptoms (Golaz et al., 1992) or in cases with Guamanian amyotrophic lateral sclerosis/Parkinsonism-dementia (Hof and Perl, 2002). Finally, a recent investigation has shown the presence of inclusion bodies comparable to Bunina bodies in the Betz cells of aged normal human brains, and also reported that some Betz cells contain lamellar inclusions (Sasaki and Iwata, 2001). We did not investigate the presence of such inclusion bodies in our materials. However, if these inclusions occur consistently in normal human brains, they could be used as an additional specific marker of Betz cells during aging.

In conclusion, our study shows that Betz cells exhibit a characteristic distribution in the human primary motor cortex that is likely related to their possible function in control of hand movements and antigravity musculature. Further investigations are needed to better define the organization of functional subareas within the primary motor cortex. The results will further our understanding of the evolution of these highly specialized neurons, and help researchers develop refined clinicopathological correlations in the study of normal brain aging, amyotrophic lateral sclerosis, and other neurodegenerative disorders with motor cortex involvement, such as progressive supranuclear palsy, corticobasal degeneration, and Guamanian amyotrophic lateral sclerosis/Parkinsonism-dementia complex.

ACKNOWLEDGMENTS

We thank M. Surini-Demiri and A.P. Leonard for expert technical assistance, and Drs. E. Kövari, D.P. Perl, and J.H. Morrison for helpful discussions. Dr. W.G. Young developed the NeuroZoom software, and C. Schmitz and E.A. Nimchinsky provided valuable advice on stereology and Betz cell identification. P.R. Hof is the Regenstreif Professor of Neuroscience. This work fulfills in part the requirements for C.B. Rivara's Doctor of Medicine degree at the University of Geneva, Switzerland.

LITERATURE CITED

Amunts K, Malikovic A, Mohlberg H, Schormann T, Zilles K. 2000. Brodmann's areas 17 and 18 brought into stereotaxic space—where and how variable? NeuroImage 11:66–84.

Arnold SE, Hyman BT, Flory J, Damasio AR, Van Hoesen GW. 1991. The topographical and neuroanatomical distribution of neurofibrillary tangles and neuritic plaques in the cerebral cortex of patients with Alzheimer's disease. Cereb Cortex 1:103–116.

Bailey P, von Bonin G. 1951. The isocortex of man. Urbana: University of Illinois Press. 301 p.

Betz K. 1874. Anatomischer Nachweis zweier Gehirnzentra. Zentralbl Med Wiss 12:578–580, 595–599.

Blinkov SM, Glezer II. 1968. The human brain in figures and tables. A quantitative handbook. New York: Plenum. 482 p.

Boroojerdi B, Foltys H, Krings T, Spetzger U, Thron A, Topper R. 1999. Localization of the motor hand area using transcranial magnetic stimulation and functional magnetic resonance imaging. Clin Neurophysiol 110:699–704.

Braak H. 1980. Architectonics of the human telencephalic cortex. Berlin: Springer. 147 p.

Braak H, Braak E. 1976. The pyramidal cells of Betz within the cingulate and precentral gigantopyramidal field in the human brain. A Golgi and pigmentarchitectonic study. Cell Tissue Res 172:103–119.

Brodmann K. 1903. Beiträge zur histologischen Lokalisation der Grosshirnrinde. I. Mitteilung: die Regio rolandica. J Psychol Neurol 2:79–107.

Brodmann K. 1905–1906. Beiträge zur histologischen Lokalisation der Grosshirnrinde. V. Mitteilung: über die allgemeinen Bauplan des Cortex palii bei den Mammalieren und zwei homologe Rindenfelder imbesonderen. Zugleich ein Beitrag zur Furchenlehre. J Psychol Neurol 6:275–400.

Brodmann K. 1909. Vergleichende Lokalisationslehre des Grosshirnrinde in ihren Prinzipien auf Grund des Zellenbaues. Leipzig: Barth. 324 p.

Bussière T, Gold G, Kövari E, Giannakopoulos P, Bouras C, Perl DP, Morrison JH, Hof PR. 2003. Stereologic analysis of neurofibrillary tangle formation in prefrontal cortex area 9 in aging and Alzheimer's disease. Neuroscience (in press).

Campbell AW. 1905. Histological studies on the localization of cerebral function. London: Cambridge University Press. 360 p.

Conel L. 1941. The postnatal development of the human cerebral cortex, Vol. II. Cambridge: Harvard University Press.

Davison C. 1941. Amyotrophic lateral sclerosis: origin and extent of upper motor neuron lesion. Arch Neurol 46:1039–1056.

Duyckaerts C, Godefroy G. 2000. Voronoi tessellation to study the numerical density and the spatial distribution of neurons. J Chem Neuroanat 20:83–92.

Eisen A, Kim S, Pant B. 1992. Amyotrophic lateral sclerosis (ALS): a phylogenetic disease of the corticomotoneuron? Muscle Nerve 15: 219–228.

Evarts EJ. 1965. Relation of discharge frequency to conduction velocity in pyramidal tract neurons. J Neurophysiol 28:216–228.
Evarts EJ. 1967. Representation of movements and muscles by pyramidal tract neurons of the precentral motor cortex. In: Yahr MD, Purpura DP, editors. Neurophysiological basis of normal and abnormal motor activities. New York: Raven Press. p 215–253.
Filimonoff IN. 1932. Über die Variabilität der Grosshirnrindenstruktur. Mitteilung II — Regio occipitalis beim erwachsenen Menschen. J Psychol Neurol 44:2–96.
Fujita Y, Okamoto K, Sakurai A, Amari M, Nakazato Y, Gonatas NK. 1999. Fragmentation of the Golgi apparatus of Betz cells in patients with amyotrophic lateral sclerosis. J Neurol Sci 163:81–85.
Geyer S, Ledberg A, Schleicher A, Kinomura S, Schormann T, Bürgel U, Klingberg T, Larsson J, Zilles K, Roland PE. 1996. Two different areas within the primary motor cortex of man. Nature 382:805–807.
Geyer S, Schleicher A, Zilles K. 1999. Areas 3a, 3b, and 1 of human primary somatosensory cortex: 1. Microstructural organization and interindividual varibility. Neuroimage 10:63–83.
Geyer S, Matelli M, Luppino G, Zilles K. 2000. Functional neuroanatomy of the primate isocortical motor system. Anat Embryol (Berl) 202:443–474.
Glezer II. 1959. Quantitative characteristics of certain stages of development of the cortex of the frontal lobe in human postnatal ontogenesis. In: Proceeding of the third conference on age physiology, morphology, and biochemistry. Moscow: Medgiz. p 387–394.
Golaz J, Bouras C, Hof PR. 1992. Motor cortex involvement in presenile dementia: report of a case. J Geriatr Psychiatry Neurol 5:85–92.
Gredal O, Pakkenberg H, Karlsborg M, Pakkenberg B. 2000. Unchanged total number of neurons in motor cortex and neocortex in amyotrophic lateral sclerosis: a stereological study. J Neurosci Methods 95:171–176.
Hammarberg C. 1895. Studien über Klinik und Pathologie der Idiotie nebst Untersuchungen über die normale Anatomie der Hirnrinde. Nova Acta Reg Soc Sci Upsala Ser III:1–126.
Hammer RPJ, Tomiyasu U, Scheibel AB. 1979. Degeneration of the human Betz cell due to amyotrophic lateral sclerosis. Exp Neurol 63:336–346.
Hof PR, Bouras C, Morrison JH. 1999. Cortical neuropathology in aging and dementing disorders: neuronal typology, connectivity, and selective vulnerability. In: Peters A, Morrison JH, editors. Cerebral cortex, Vol. 14, Neurodegenerative and age-related changes in cerebral cortex. New York: Kluwer Academic-Plenum. p 175–312.
Hof PR, Duan H. 2001. Age-related morphologic alterations in the brain of Old World and New World anthropoid monkeys. In: Hof PR, Mobbs CV, editors. Functional neurobiology of aging. San Diego: Academic Press. p 435–446.
Hof PR, Perl DP. 2002. Neuropathologic changes in the primary motor cortex in Guamanian amyotrophic lateral sclerosis/parkinsonism-dementia complex. Neurosci Lett 328:294–298.
Hore J, Porter R. 1972. Pyramidal and extrapyramidal influences on some hindlimb motoneuron populations of the arboreal bush-tailed possum, *Trichosurus vulpecula*. J Neurophysiol 35:112–121.
Howard CV, Reed MG. 1998. Unbiased stereology—three dimensional measurement in microscopy. New York: Springer. 246 p.
Kaiserman-Abramof IR, Peters A. 1972. Some aspects of the morphology of Betz cells in the cerebral cortex of the cat. Brain Res 43:527–546.
Kaplan LL. 1952. Development of the giant pyramidal cells of the motor cortex of the brain in a series of mammals. Arkh Anat Gistol Embriol 2:18.
Kiernan JA, Hudson AJ. 1991. Changes in sizes of cortical and lower motor neurons in amyotrpohic lateral sclerosis. Brain 114:843–853.
Lassek AM. 1939. The human pyramidal tract. I. A fiber and numerical analysis. Arch Neurol Psychiatry 42:872–876.
Lassek AM. 1940. The human pyramidal tract. II. A numerical investigation of the Betz cells of the motor area. Arch Neurol Psychiatry 46:718–724.
Lassek AM. 1954. The pyramidal tract. Springfield: Charles C. Thomas. 166 p.
Lassek AM, Wheatley WD. 1945. An enumeration of the large motor cells of area 4 and the axons of the pyramids of the chimpanzee. J Comp Neurol 82:299–302.
Lawyer T Jr, Netsky MG. 1953. Amyotrophic lateral sclerosis: clinicoanatomic study of 53 cases. Arch Neurol 69:171–192.
Lewis WB. 1878. On the comparative structure of the cortex cerebri. Brain 1:79–96.
Lewis WB, Clarke H. 1878. The cortical lamination of the motor area of the brain. Proc R Soc Lond 27:38–49.
Lundberg A, Voorhoeve P. 1962. Effects from the pyramidal tract on spinal reflex arcs. Acta Physiol Scand 56:201–219.
Marie P. 1928. Travaux et mémoires, Vol. 2. Paris: Masson.
Meyer G. 1987. Forms and spatial arrangement of neurons in the primary motor cortex of man. J Comp Neurol 262:402–428.
Murayama S, Bouldin TW, Suzuki K. 1992. Immunohistochemical and ultrastructural studies of upper motor neurons in amyotrophic lateral sclerosis. Acta Neuropathol (Berl) 83:518–524.
Nakamura S, Akiguchi I, Kameyama M, Mizuno N. 1985. Age-related changes of pyramidal cell basal dendrites in layers III and V of human motor cortex: a quantitative Golgi study. Acta Neuropathol (Berl) 65:281–284.
Nihei K, McKee AC, Kowall NW. 1993. Patterns of neuronal degeneration in the motor cortex of amyotrophic lateral sclerosis patients. Acta Neuropathol (Berl) 86:55–64.
Nimchinsky EA, Hof PR, Perl DP, Morrison JH. 1992. The frontal cortex in neurodegenerative disorders: cellular and regional patterns of vulnerability. Abstr Soc Neurosci 18:557.
Nimchinsky EA, Young W, Yeung G, Shah RA, Gordon JW, Bloom FE, Morrison JH, Hof PR. 2000. Differential vulnerability of oculomotor, facial and hypoglossal nuclei in G86R superoxide dismutase transgenic mice. J Comp Neurol 416:112–125.
Page TL, Einstein M, Duan H, He Y, Flores T, Rolshud D, Erwin JM, Wearne SL, Morrison JH, Hof PR. 2002. Morphological alterations in neurons forming corticocortical projections in the neocortex of aged patas monkeys. Neurosci Lett 317:37–41.
Pakkenberg B, Gundersen HJG. 1997. Neocortical neuron number in humans: effect of sex and age. J Comp Neurol 384:312–320.
Pamphlett R, Kril J, Hng TM. 1995. Motor neuron disease: a primary disorder of corticomotoneurons? Muscle Nerve 18:314–318.
Penfield W, Rasmussen T. 1950. The cerebral cortex of man. New York: Macmillan. 248 p.
Perl DP, Good PF, Bussière T, Morrison JH, Erwin JM, Hof PR. 2000. Practical approaches to stereology in the setting of aging- and disease-related brain banks. J Chem Neuroanat 20:7–19.
Pizzella V, Tecchio F, Romani GL, Rossini PM. 1999. Functional localization of the sensory hand area with respect to the motor central gyrus knob. NeuroReport 10:3809–3814.
Preston JB, Shende MC, Uemura K. 1967. The motor cortex-pyramidal system: patterns of facilitation and inhibition on motoneurons innervating limb musculature of cat and baboon and their possible adaptive significance. In: Yahr MD, Purpura DP, editors. Neurophysiological basis of normal and abnormal motor activities. New York: Raven Press. p 61–72.
Rademacher J, Caviness VS Jr, Steinmetz H, Galaburda AM. 1993. Topographical variation of the human primary cortices: implications for neuroimaging, brain mapping, and neurobiology. Cereb Cortex 3:313–319.
Rademacher J, Bürgel U, Geyer S, Schormann T, Schleicher A, Freund HJ, Zilles K. 2001. Variability and assymetry in the human precentral motor system. A cytoarchitectonic and myelocytoarchitectonic brain mapping study. Brain 124:2232–2258.
Sanides F. 1962. Die Architektonik des menschlichen Stirnhirns. In: Müller M, Spatz H, Vogel P, editors. Monographien der Gesamtgebieten der Neurologie und Psychiatrie, Vol. 98. Berlin: Springer. 247 p.
Sanides F. 1972. Representation in the cerebral cortex and its areal lamination patterns. In: Bourne GH, editor. The structure and function of the nervous tissue, Vol. 5. New York: Academic Press. p 329–453.
Sasaki S, Iwata M. 1999. Ultrastructural change of synapses of Betz cells in patients with amyotrophic lateral sclerosis. Neurosci Lett 268:29–32.

Sasaki S, Iwata M. 2001. Ultrastructural study of Betz cells in the primary motor cortex of the human brain. J Anat 199:699–708.

Sasaki S, Maruyama S. 1994. Immunocytochemical and ultrastructural studies of the motor cortex in amyotrophic lateral sclerosis. Acta Neuropathol (Berl) 87:578–585.

Scheibel ME, Tomiyasu U, Scheibel AB. 1977. The aging human Betz cell. Exp Neurol 56:598–609.

Scheibel ME, Scheibel AB. 1978. The dendritic structure of the human Betz cell. In: Brazier MAB, Pets H, editors. Architectonics of the cerebral cortex. New York: Raven Press. p 43–57.

Schleicher A, Amunts K, Geyer S, Kowalski T, Schormann T, Palomero-Gallhager N, Zilles K. 2000. A stereological approach to human cortical architecture: identification and delineation of cortical areas. J Chem Neuroanat 20:31–47.

Schmitz C. 1998. Variation of fractionator estimates and its prediction. Anat Embryol (Berl) 198:371–397.

Schmitz C, Schuster D, Niessen P, Korr H. 1999. No difference between estimated mean nuclear volumes of various types of neurons in the mouse brain obtained on either isotropic uniform random sections or conventional frontal or sagittal sections. J Neurosci Methods 88:71–82.

Schmitz C, Hof PR. 2000. Recommendations for straightforward and rigorous methods of counting neurons based on a computer simulation approach. J Chem Neuroanat 20:93–114.

Smith GE. 1907. A new topographical survey of the human cerebral cortex, being an account of the distribution of the anatomically distinct cortical areas and their relationship to the cerebral sulci. J Anat 41:237–254.

Takahashi K. 1965. Slow and fast groups of pyramidal tract cells and their respective membrane properties. J Neurophysiol 28:908–924.

Takahashi N, Kawamura M, Araki S. 2002. Isolated hand palsy due to cortical infarction: localization of the motor hand area. Neurology 58:1412–1414.

Tigges J. 1992. Novel inclusion bodies in Betz cells of cortical area 4 of aged Rhesus monkeys. Anat Rec 233:162–168.

Tigges J, Herndon JG, Peters A. 1992. Axon terminals on Betz cell somata of area 4 in Rhesus monkey through adulthood. Anat Rec 232:305–315.

Tsuchiya K, Ozawa E, Haga C, Watabiki S, Ikeda M, Sano M, Ooe K, Taki K, Ikeda K. 2000. Constant involvement of the Betz cells and pyramidal tract in multiple system atrophy: a clinicopathological study of seven autopsy cases. Acta Neuropathol (Berl) 99:628–636.

Tsuchiya K, Ikeda M, Mimura M, Takahashi M, Miyazaki H, Anno M, Shiotsu H, Akabane H, Niizato K, Uchihara T, Tominaga I, Nakano I. 2002. Constant involvement of the Betz cells and pyramidal tract in amyotrophic lateral sclerosis with dementia: a clinicopathologic study of eight autopsy cases. Acta Neuropathol (Berl) 104:249–259.

Udaka K, Kameyama M, Tomonaga M. 1986. Degeneration of Betz cells in motor neuron disease. A Golgi study. Acta Neuropathol (Berl) 70:289–295.

Vogt C, Vogt O. 1926. Die vergleichend-architektonische und die vergleichend-reizphysiologische Felderung der Grosshirnrinde unter besonderer Berücksichtigung der menschlichen. Naturwissenschaften 14:1190–1194.

Vogt O. 1910. Die myeloarchitektonische Felderung des menschlichens Stirnhirns. J Psychol Neurol 15:221–232.

von Bonin G. 1949. Architecture of the precentral motor cortex and some adjacent areas. In: Bucy PC, editor. The precentral motor cortex. Urbana: University of Illinois Press. p 7–82.

von Economo C, Koskinas G. 1925. Die Cytoarchitektonik der Hirnrinde des erwachsenen Menschen. Berlin: Springer. 804 p.

Walshe FM. 1942. The giant cells of Betz, the motor cortex and the pyramidal tract: a critical review. Brain 65:409–461.

Welker WI, Campos GB. 1963. Physiological significance of sulci in somatosensory cerebral cortex in mammals of the family Procyonidae. J Comp Neurol 120:19–36.

West MJ, Slomianka L, Gundersen HJG. 1991. Unbiased stereological estimation of the total number of neurons in the subdivisions of the rat hippocampus using the optical fractionator. Anat Rec 231:482–497.

White LE, Andrews TJ, Hulette C, Richards A, Groelle M, Paydarfar J, Purves D. 1997a. Structure of the human sensorimotor system. I: Morphology and cytoarchitecture of the central sulcus. Cereb Cortex 7:18–30.

White LE, Andrews TJ, Hulette C, Richards A, Groelle M, Paydarfar J, Purves D. 1997b. Structure of the human sensorimotor system. II: Lateral symmetry. Cereb Cortex 7:31–47.

Wise SP. 1985. The primate premotor cortex: past, present and preparatory. Annu Rev Neurosci 8:1–19.

Young WG, Nimchinsky EA, Hof PR, Morrisson JH, Bloom FE. 1997. NeuroZoom software user guide and reference book. San Diego: YBM, Inc. 1038 p.

Yousry TA, Schmid UD, Alkadhi H, Schmidt D, Peraud A, Buettner A, Winkler P. 1997. Localization of the motor hand area to a knob on the precentral gyrus. A new landmark. Brain 120:141–157.

Zeki S. 1979. Zu Brodmanns area 18 und area 19. Exp Brain Res 36:195–197.

Zilles K. 1990. Cortex. In: Paxinos G, editor. The human nervous system. San Diego: Academic Press. p 757–852.

Zilles K, Schleicher A, Langenmann C, Amunts K, Morosan P, Palomero-Gallhager N, Schormann T, Mohlberg H, Bürgel U, Steinmetz H, Schlaug G, Roland PE. 1997. Quantitative analysis of sulci in the human cerebral cortex: development, regional heterogeneity, gender difference, asymmetry, intersubject variability and cortical architecture. Hum Brain Mapp 5:218–221.